J. Mol. Model. **1998**, *4*, 61 – 72

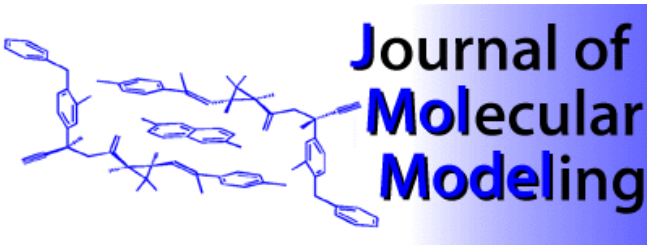

FULL PAPER

Pentagonal Model of Membrane Channel of Na,K-ATPase. Computer Simulations of Structure and Electrostatic Properties

Viktor B. Luzhkov and Nikolai F. Surkov

Institute of Chemical Physics in Chernogolovka, Russian Academy of Science, Chernogolovka, Moscow region, Russia, 142432. E-mail: luzhkov@icp.ac.ru

Received: 5 December 1997 / Accepted: 26 January 1998 / Published: 13 February 1998

Abstract Computational modeling of the membrane channel of a sodium pump (Na,K-ATPase) is performed and the role of selected amino acids in binding of sodium ions is discussed. The channel is build as a pentameric 10-helix bundle. The transmembrane a-helices are determined from hydropathy calculations. The spatial arrangement of transmembrane a-helices is chosen according to the size of a pore, intersegment loops geometry, and orientation hydrophobicities of transmembrane segments. The latter property provides the numerical estimate of the distribution of the hydrophobic properties at the helical wheels. The model system involves the peptide part and 150 water molecules that soak the pore. The channel structure is submitted to geometry minimization and molecular dynamics relaxation. The relative stability of the channel states with the negatively charged acidic residues belonging to the pore interior decrease in the order Glu-334 > Asp-810 > Glu-785 > Asp-814. The estimated binding energies of 1-3 Na^+ ions with the channel with the ionized Glu-334 and Glu-785 amino acids are in the range allowing the exothermic complexation.

Keywords Na,K-ATPase , Hydropathy calculations, Molecular Modeling, Molecular Dynamics, Ion transport

Introduction

Na,K-ATPase, or just sodium pump, is an important membrane protein involved in an active transport of Na^+ and K^+ ions in most animal cells. Much attention was given to the studies of molecular mechanisms of its transport activity, and particularly to disclosure of its 3-D structure [1-4]. The only existing low-resolution structural data support the 'one subunit' structure of membrane channel part, but unfortunately provide little information about the fine features of the spatial arrangement of Na,K-ATPase [2b]. Thus far, an extensive experimental data on protein topology is available [5-9]. The intracellular location of N- and C-termini and the amino acid sequences of several extracellular and cytoplasmic protein regions are established [8]. The existing data support either 8 or 10 transmembrane segment structure of the α-subunit of Na,K-ATPase with the latter number being more plausible [6c, 8c, 9]. Point mutation studies revealed an important role of several Glu and Asp amino acids in channel permeability [7,9-11]. But still a major lack of exact structural information for this protein does not al-

Correspondence to: V. B. Luzhkov

low unambiguous interpretation of much of 'structure-function' data.

The theoretical interpretations of structural organization of membrane proteins significantly progressed recently [12,13]. Particularly, a number of computational studies revealed important structural properties of membrane ion channels [14]. Similar to voltage- and ligand- gated ion channels, the sodium pump is involved in the ion transport across membrane. But unlike the passive transporters where the channels pore could be expected to have a rigid structure, the sodium pump is an active transporter where the conformational changes are expected to be deeper. The only known attempt of building the spatial model of membrane part of Na,K-ATPase [4] was based on global optimization of hydrophobic and steric interactions between transmembrane helical segments for 8 and 10 segments architectures of the channel. The 'bakteriorhodopsin-like' tight assembly of the helices had resulted from that calculations where the polar residues are evenly spread in the space of the protein and no distinct ion channel opening could be viewed. This makes the model of Modyanov [4] look unrealistic since the binding of several ions could require noticeable space within the transmembrane part of the protein. The experimental data support the general model of Na,K-ATPase where its transport activity proceeds in a cyclic manner between two major E1 and E2 conformations [1,3]. E1 conformation is responsible for binding 3 intracellular Na^+ , while E2 - for binding 2 extracellular K^+ ions. In principle, E1 and E2 conformations could correspond to a very different protein spatial configurations. The restriction is that the energy cost for the transition between them should not exceed the energy of hydrolysis of 1 ATP molecule consumed per one cycle of the pump action. Considering the protein structures having the minimal conformational differences between E1 and E2 states it is straightforward to assume the existence of a membrane channel (MC) common to both conformations and open either to cytoplasmic or periplasmic side of biomembrane, respectively. The structure of this channel could be subjected only to minor conformational changes coupled with the ATP hydrolysis. The computer generated pentameric model of the Na,K-ATPase channel was proposed recently [15]. The present work provides the analysis of its structure and electrostatic properties associated with the binding of Na^+ ions.

Methodology

The membrane part of the α-subunit of Na,K-ATPase is modeled as a bundle of α-helices with an equal length. The major steps in building of MC model involve estimation of putative membrane spanning helices, selection of the channel architecture and the corresponding arrangement of the transmembrane segments. Amino acid sequence of Na,K-ATPase from Torpedo Californica [16] is taken for modeling. The transmembrane segments predicted from hydropathy calculations using the Goldman-Engelman-Steitz (GES) amino acid polarity scale [17] are taken for building the model. The averaging window of 21 residue is used since the 30 Å height of the corresponding α-helical cylinder is close to an assumed membrane width. The GES calculated transmembrane domains are verified using Dense Alignment Surface (DAS) method [18] at the Expasy Web site [19]. Multiple alignment of amino acid sequences of different α-subunit isoforms of Na,K-ATPase extracted from the SWISS-PROT data bank [19] is performed using Multalin program [20] as the Expasy Web site tool.

Computer simulations of MC structure are performed using molecular modeling tools of the INSIGHT II program [21]. The building of channel structure involves generating the structures of isolated transmembrane segments with an ideal α-helical geometries, followed by rotamer search for

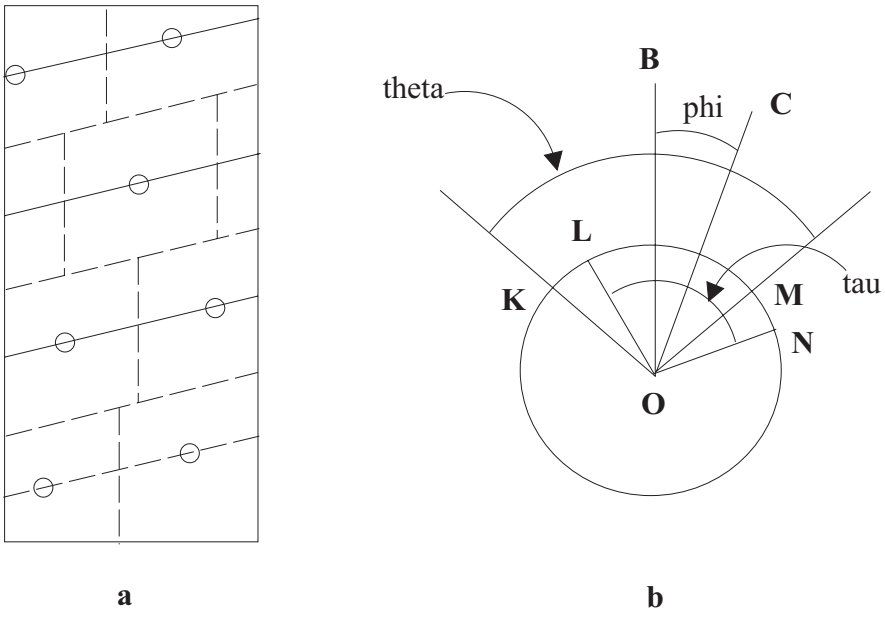

Figure 1 **a***) Side-view of an α-helix cylinder and the surface elements of individual amino acids.* **b***) Top-view of an alpha-helical cylinder. Arc KM (angle θ) corresponds to the part of cylinder that is exposed into the pore. Arc LN (angle τ) presents projection of the surface element of individual amino acid and arc LM presents the part of this element that is exposed into the pore. BOC (ϕ) is the angle between the central lines of sectors KM and LN.*

the most stable side-chain-conformations and a full geometry minimization of each α-helical segment. The initial channel's structure is manually assembled from the optimized α-helices according to the predetermined architecture where five most hydrophilic α-helices are taken to form the channel's pore.

The starting mutual orientations of the inner helices are chosen from the estimates of hydrophobic properties of the portions of their surfaces exposed to the pore, *orientation hydrophobicities* . These calculations are performed in approximation where amino acids are presented as regions of equal area at the helical cylinder (Fig.1a). The numeric procedure [22] is based on the estimate of the hydrophobicity of the angular sector θ at the surface of the helical cylinder (arc KM at Fig.1b) that scans the helical wheel of a given α-helix in the rotation angle range ϕ= 0-360 grad. In this respect it has the analogy with the common hydropathy analysis that calculates the integral hydrophobicity in a moving window that scans amino acid sequence. The angle θ of the scanning angle sector corresponds to the portion of the helical wheel that is exposed to the pore. The value of orientation hydrophobicity is given by the sum of contributions from individual amino acids, which are given by symmetric S-shaped functions. For a given value of ϕ the non-zero contributions come only from amino acids that are visible from the pore. The S-shaped functional form accounts for the change of the visible area (arc LM) of amino acid region (arc LN, angle τ) with respect to rotation angle ϕ and for anisotropic distribution of local hydrophobicity at amino acids regions. The amplitudes of individual S-functions correspond to amino acid hydropathy indexes from GES scale [17]. For a regular pentameric pore the angles τ and θ possess an approximately equal values, 100 and 104 grad, respectively. The calculated distributions of orientation hydrophobicities provide qualitatively correct estimates of the positions of transmembrane helices with respect to the pore for the ion channels with a well characterized structure like nicotinic acetylcholine receptor, cholera toxin B, phosphalamban [22].

After generating initial channel structure its pore is soaked with water molecules. The structure of this cluster is submitted to energy minimization and molecular dynamics equilibration. The total number of atoms in the modeled systems (in a neutral state, in the states with ionized Glu and Asp amino acid residues and with bound Na^+ ions) equals 3804-3812. Potential energies are calculated using Biosym's Consistent Valence Force Field [23]. A group-based technique with a 20 Å cutoff distance is employed for nonbonded interactions. Minimizations of molecular structure start with a steepest-descent algorithm (convergence criteria 100 $kcal \cdot mol^{-1} \cdot Å^{-1}$) and are followed at convergence of the first step by Polak-Rubiere conjugate gradient optimization method (convergence threshold of 0.01 $kcal \cdot mol^{-1} \cdot Å^{-1}$). The MD simulations are performed at 298 K (NVT statistical ensemble) with a time step of 2 fs and using the Rattle algorithm for bond constraints. The MD runs have 60 ps duration with 20 ps for equilibration stage and 40 ps for data collection stage.

In course of geometry minimization and MD calculations a set of distance restraints is imposed to enforce the system to stay in accord with its initial architecture. A flat-bottomed restraint potential is used to keep the distances between the axes of adjacent helices within 9.5-11.5 Å range, that is characteristic for membrane proteins [12,14]. This was implemented by putting 3 dummy atoms (for each helix) in the beginning, in the middle, and in the end of the given helix axis. The distances between the neighbor dummy atoms of adjacent helices were controlled in course of MD calculations. Additionally the backbone structures (CA atom positions) of 5 outer helical segments are kept fixed during MD simulations. These types of restraints keep the distances between the centers of helices within the given range but allow the mutual rotations between helices and minor shifts be-

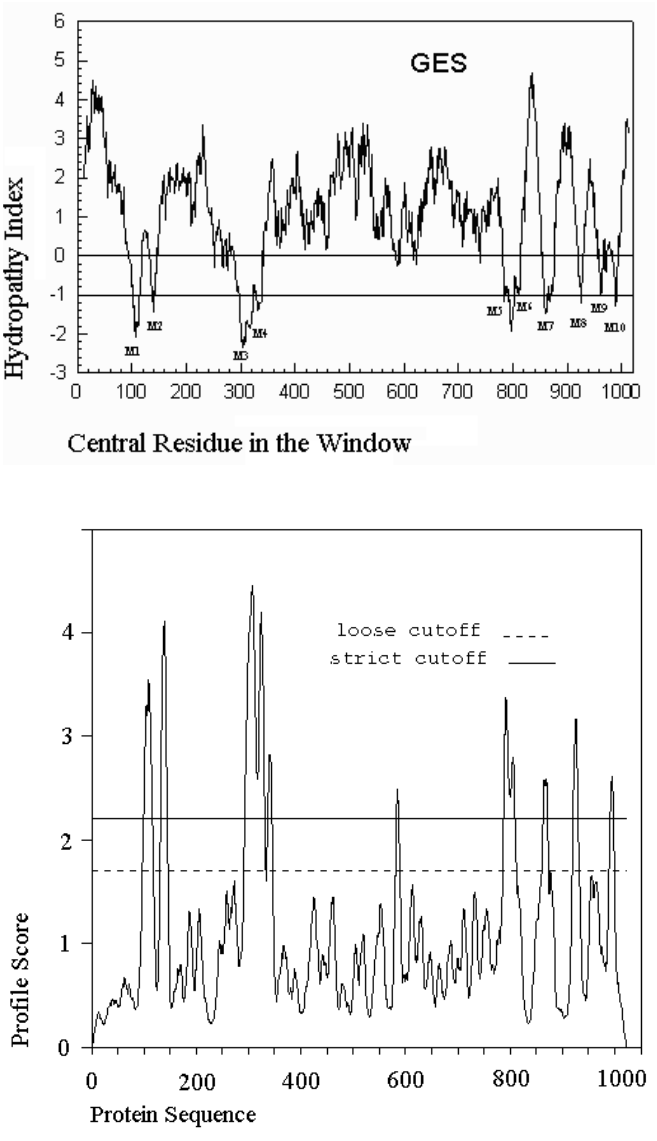

Figure 2 *GES hydropathy data for the α-subunit of Na,K-ATPase (top). Transmembrane segment profile score from DAS calculations (bottom)*

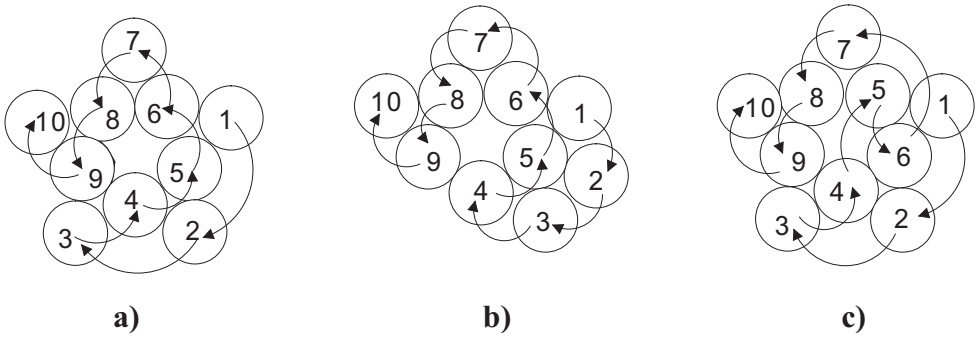

Figure 3 *Selected arrangements of 10 transmembrane helices of Na,K-ATPase*

tween them. Besides, the water molecules are restrained to stay within the pore.

The binding energies of Na^+ ions , ΔE_{bind} ,are calculated using the general formula for the energy of forming the molecular complexes

$$\Delta E_{bind} = 0.5\ \Delta E_{el} + \Delta E_{vdw} + \Delta E_{int} \quad (1)$$

where ΔE_{el}, ΔE_{vdw} and ΔE_{int} terms refer to the differences in electrostatic, van der Waals and internal energies of the bound and unbound systems, respectively. It is important to note the use of the scaling coefficient 0.5 at electrostatic term, which comes from linear response approximation [24] and which is erroneously omitted sometimes in ion binding calculations.

Results

Building the model

Predicted membrane spanning α-helices are given in Table 1. In general an identification of transmembrane segments using hydropathy data depends on the hydrophobic cut-off level as well as on the window size. The logic of building the model as a bundle of helices of an equal length forces us to use a fixed size of the window (21 residue). The corresponding hydropathy plot using GES scale is given at Fig.2a. Nine distinct and separated by more than 21 residue minimums corresponding to the hydrophobic stretches are found at -1.0 cutoff level. The broad hydrophobic peak in the region of 800 could be considered as a double transmembrane stretch with minor peaks at 785 and 811 positions. The corresponding intersegment loop at 796-800 positions contains a polar Asn-796 residue and two Pro-798,800 residues that are characteristic to β-turns. Calculations using DAS method also predict similar hydrophobic domains (Table 1), except that the M5 and M6 helices are shown as one long segment and M9 helice corresponds to the peak at 1.6 score level (Fig.2b) that is slightly lower than 1.7 cutoff value. The transmembrane sequences predicted in calculations of ref. [25] using an optimized form of hydropathy descriptor and a variable size of averaging window are similar to the sequences calculated in this work. Thus the present analysis of the hydropathy data coming from several different methods supports the existence of 10 transmembrane segments which completely agrees with the experimental data on tryptic digestion [6], epitope binding [8], and point mutations [10] in Na,K-ATPase. The measured exposed regions of protein sequence do not overlap with the transmembrane α-helices. Several extra possible membrane spanning domains follow from DAS calculations and from ref. [25], but the relevant experimental data indicate that the corresponding amino acids in the range from 376 to 725 belong rather to the cytoplasmic side [7-9]. Some of the segments (namely, M4, M5, M6, M10) contain Pro residues. While the presence of the latter residue could drastically question the possibility of the α-helice formation in a globular protein, it is not so unfrequented in membrane proteins [13,26]. 10 transmembrane α- helices resulting from GES calculations are used in further modeling.

The next step involves prediction of the spatial arrangement of transmembrane stretches. The pseudo-symmetrical pentameric arrangement of 10 α-helices in the channel bundle given at Fig. 3 was proposed in ref. [15]. This choice had several grounds for it. With regard to the inner part, the pentagonal pore is the first one, after the pores made of 3 and 4 α-helices, that has an appreciable conductance for the K^+ ions in experiment [1]. The pore composed of 6 helices could be considered as a too wide opening to be selective enough in binding specifically Na^+ and K^+ ions. The pentameric structure is found also in several ion channels with a well characterized three-dimensional structure [27]. The plausible resemblance between the structural features of membrane channels of Na,K-ATPase and of nicotinic acetylcholine receptor was noticed in electron microscopy studies [2b]. The pentameric arrangement is chosen also for the peripherial

Figure 4 (next pages) *Calculated orientation hydrophobicity plots (GES scale) of the inner transmembrane segments of Na,K-ATPase and the corresponding helical wheels.* **a***) - M4,* **b***) - M5,* **c***) - M6,* **d***) - M8,* **e***) - M9 helices. Zero angle at the plots correspond to positions of the first amino acids in the given sequences. Contributions from the individual hydrophilic amino acid residues are marked at the plots, sign 'Sum' indicate the plots of resulting orientation hydrophobicity functions for a given amino acid sequences. The arrows indicate the positions of orientation hydrophilicity functions at the corresponding helical wheels.*

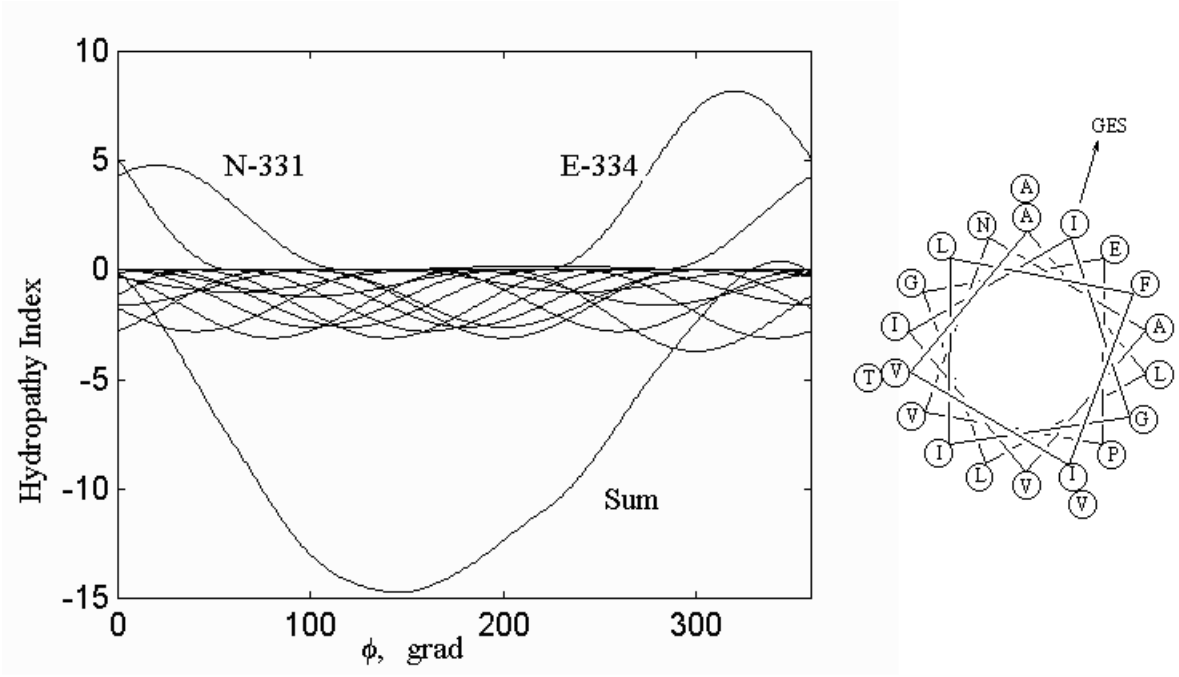

Figure 4a

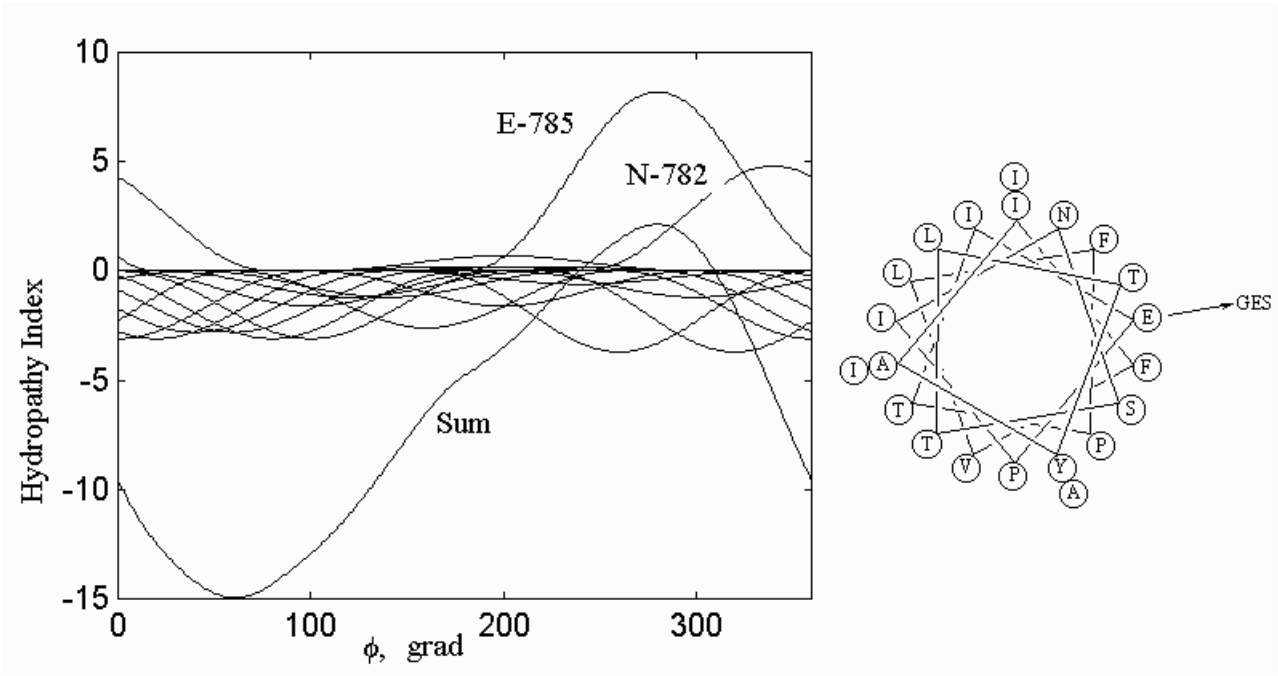

Figure 4b

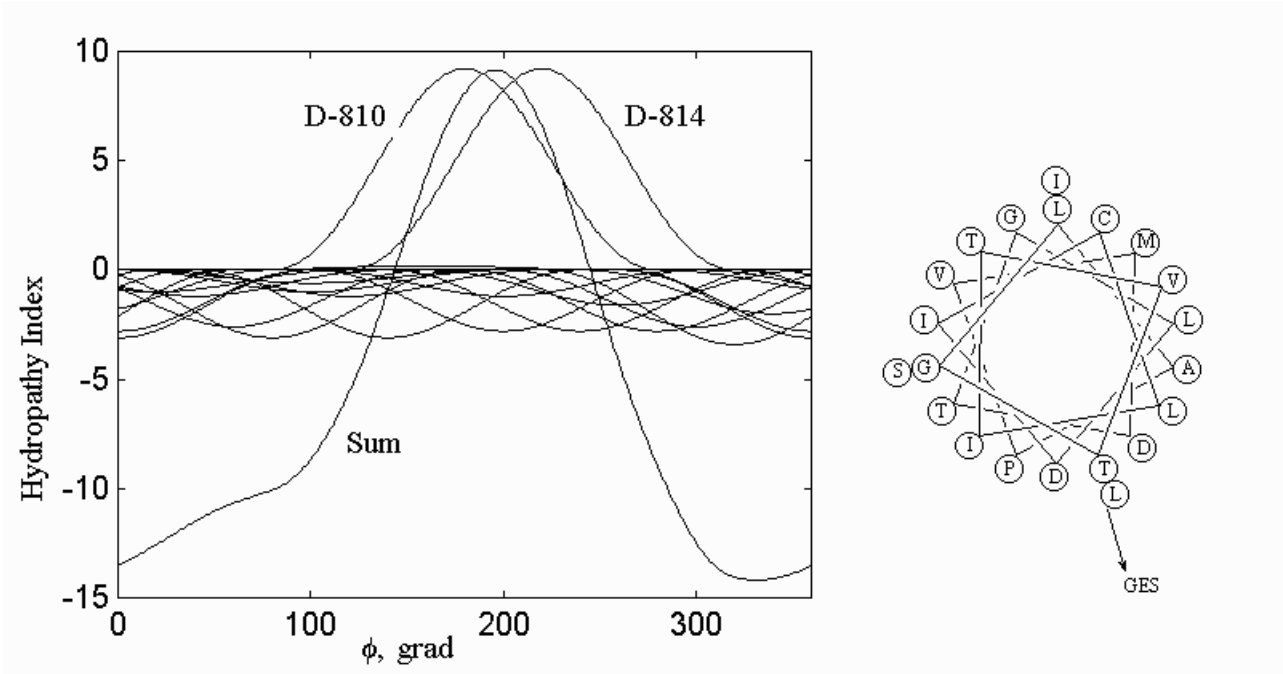

Figure 4c

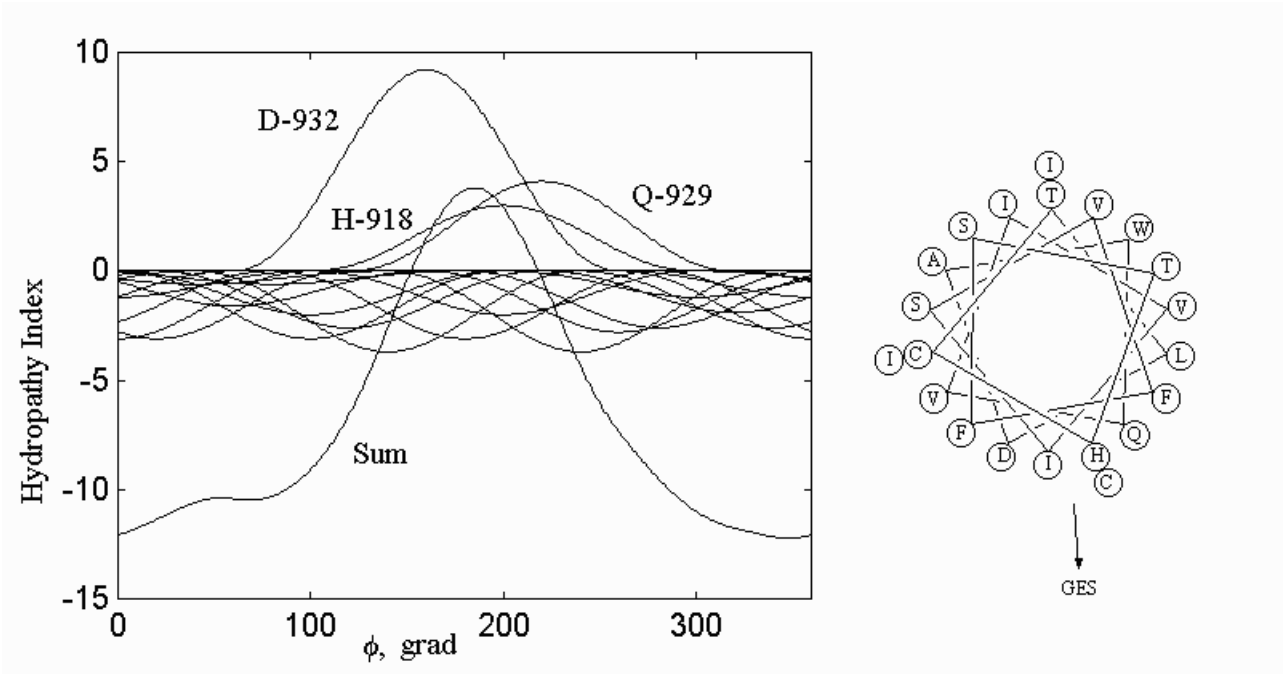

Figure 4d

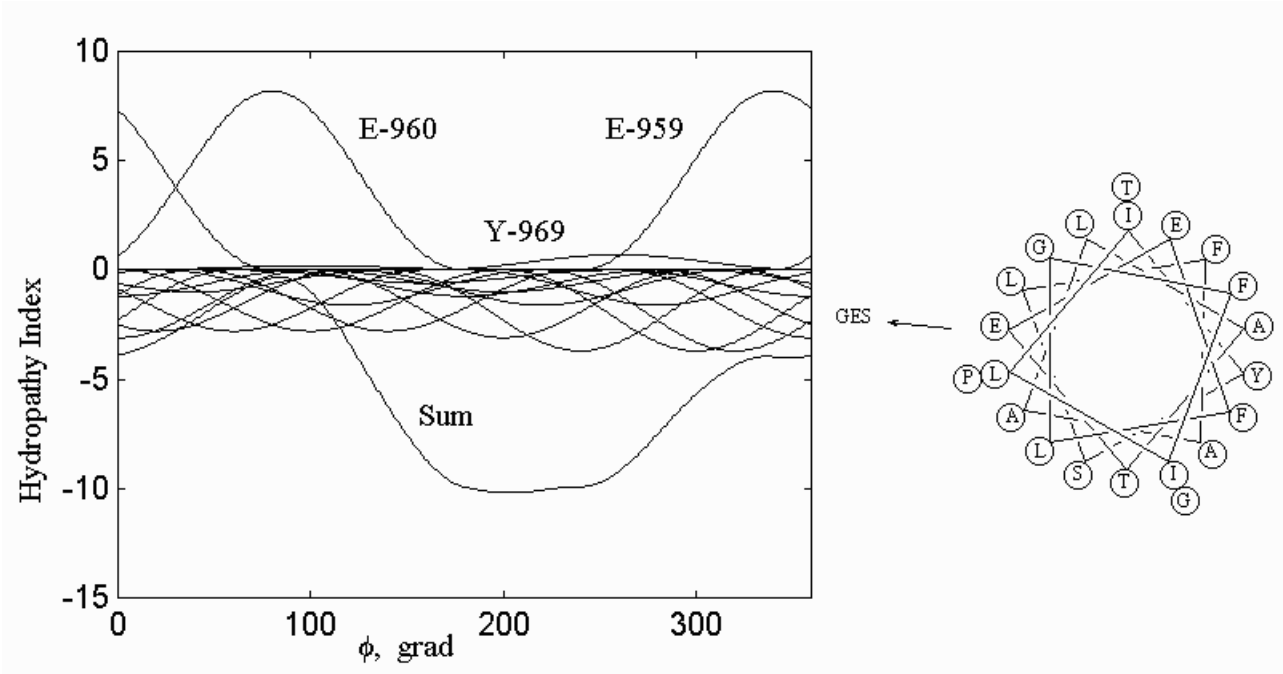

Figure 4e

transmembrane helices. The pseudo-symmetric arrangement of the helices (examples are given at Fig. 3a,c) is expected to provide the most polar environment inside the pore compared to configurations with lower symmetry (one possible structure is given at Fig. 3b) due to better screening of the pore from the nonpolar lipid media.

Next, the α-helices are positioned within the given pattern. The ion channel provides a favourable environment for the passing ions and associated water molecules. Therefore the pore is expected to be formed from 5 most hydrophilic transmembrane segments. The explicit separation in the angle orientation of hydrophobic and hydrophilic amino acids at the helical wheels could be also important for these helices. Thus we consider both the integral and orientation hydrophobicities of transmembrane domains. The rank order of the integral hydrophilicity coming from GES calculations (Table 1) is 6 > 9 > 5 > 8 > 10 > 4 > 2 > 7 > 1 > 3. The rank order of calculated oriented hydrophilicities using GES scale is 6 > 8 > 5> 4 > 10 9 > 7 > 2 > 3 > 1. The 6^{th}, 8^{th} , 5^{th} , 9^{th} , and 4^{th} segments have the highest sum of ranks and thus these α-helices are assigned to the inner part of MC as the most hydrophilic ones. All these segments contain acidic Glu and Asp amino acids, that were experimentally proven as putative transportation sites [7,9-10].

The quick check shows that there is a limited number of geometrically allowed permutations of helix positions in MC structure. These limitations are imposed by the predicted short length of intersegement loops between M3 and M4, M5 and M6, M8 and M9 helices (see amino acid numbers in Table 1) and the corresponding segments could be expected to hold adjacent positions. In principle the additional data on the interhelical positions could be obtained from the measurements of S-S links, but unfortunately the latter one belong to regulatory site [28]. Finally, additional topological restriction that the intersegment loops should not intersect each other and should not cross the opening of the pore (like for structure at Fig.3c) leaves the single arrangement of α-helices (Fig. 3a) which is considered in the further modeling.

The angular orientation of the α-helices in their cluster is the last step in building the starting structure. The straightforward approach involves extremely time-consuming conformational search of a global minimum with respect to mutual rotations of all 10 α-helices. For the inner helices M4, M5, M6, M8, and M9 we assume instead that their most hydrophilic sides are directed into the pore. These orientations are determined according to location of the most hydrophilic sites at their helical wheels. At the calculated orientation hydrophobicity plots the S-function contributions from the hydrophilic amino acids have positive amplitudes while from hydrophobic ones - negative amplitude. The maximums at the plots of orientation hydrophobicity at Fig. 4 correspond to the positions of hydrophilic acidic amino acids. Exception is the M9 helix, where the plot of orientation hydrophobicity has a relatively flat character between Glu-959,960 residues with the maximum at Glu-960. The starting orientation of M9 is taken in the way that both Glu are equally exposed to the pore. The rotation angles of outlying helices are selected to minimize the steric interactions due to bulky side chains and to achieve the most tight complex with the inner helices. The starting model presented a bundle of 10 parallel α-helices with the distances between the axes of adjacent helices in the range of 9.1-11.9 Å. The soak of the pore's interior pro-

duces 150 water molecules inside and in the 2 Å vicinity of the channel.

Useful prognosis about the tentative structure of membrane proteins could be obtained from the amino acid sequence alignment. The lipid facing amino acids tend to be more evolutionary variable than amino acids lining the pore [13]. The multiple sequence alignment of predicted membrane segments is performed for several isoforms of α-subunit of Na,K-ATPase. Isoforms of α-1, α-2 and α-3 types are considered since they are expected to have larger sequence variations than isoforms of one type [7]. A high level of homology is found for the given sequences. The sequence of Torpedo Californica is conserved at the 88% level of identity. Some nonpolar amino acids from predicted transmembrane segments show variable level of conservation, while the amino acids that belong to the pore in a given model are 100% conserved which can serve as an indirect support of the given model.

Structural and electrostatic features of the model

The starting all atom MC structure is submitted first to geometry minimization to eliminate initially too close contact interatomic distances. This is followed by 30 ps MD equilibration and subsequent geometry minimization. In the resulting structure the adjacent α-helices are slightly inclined with respect to each other (Fig.5) similar to calculated structures of other α-helical bundles [14]. The helix-to-helix separation stay within the range of applied constraints. Minor rotations of inner α-helices are observed compared to the starting structure. The side chains of Glu-334, Glu-785, Asp-810, and Asp-814 residues still stick into the pore, the side chains of Glu-959, and Glu-960 belong to the walls of a pore, while M8 helix is rotated so that the side chain of Asp-932 is directed along the pore wall towards M9 (Fig.5b).

The occlusion of several cations within the Na,K-ATPase channel can proceed only in the presence of counterions in the form of ionized acidic amino acid residues. The binding of 3 ions of Na^+ require at least 2 ionized acidic residues in the channel. The generated channel structure could be regarded as the analog of E1 conformation since it possesses the most hydrophilic configuration of the pore. In characterizing the electrostatic properties of MC the relative energies of the states with ionized Glu and Asp residues are calculated. The corresponding average potential energies from the MD runs of 60 ps duration show that the relative potential energies of carboxy anions increase in the order Glu-334 < Asp-810 (10.5) < Glu-785 (12.2) < Asp-814 (38.2) < Asp-932 (45.4). Here, in the brackets the energies (in kcal·mol) relative to most stable anion of Glu-334 are provided. The given energies reflect the stabilization of anions in their microenvironment and show that ionization of three acidic residues Glu-334, Asp-810, and Glu-785 is markedly more

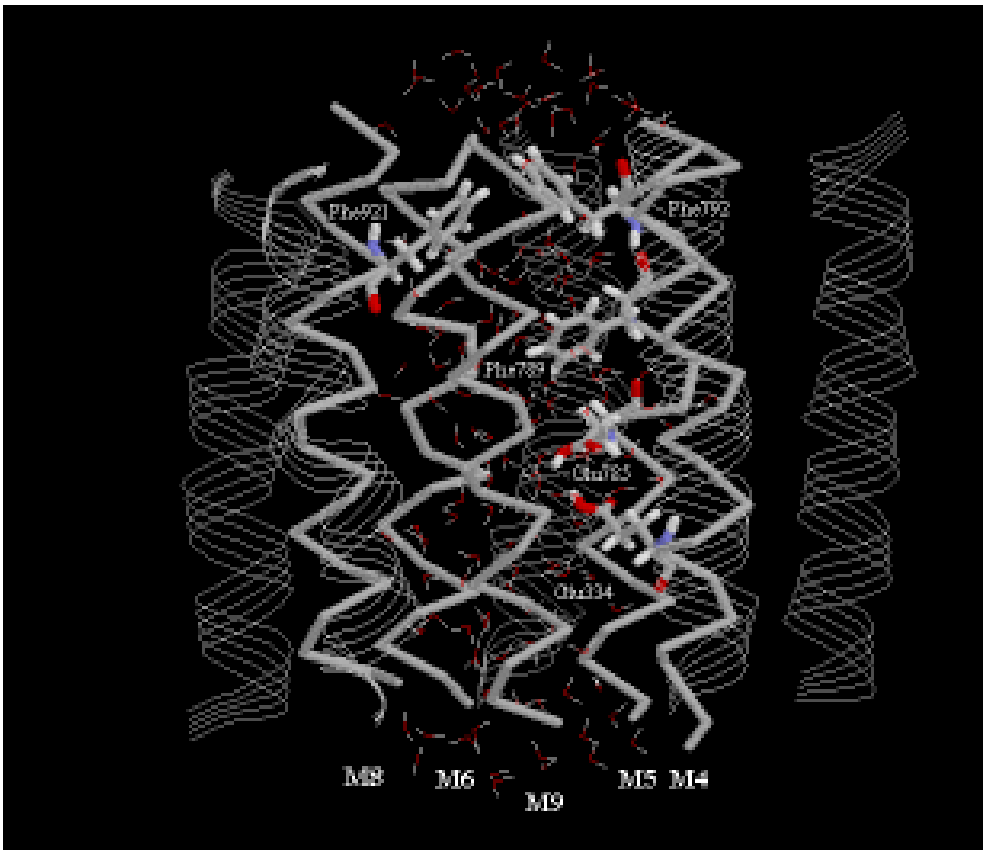

Figure 5a *Side view of equilibrated MC structure. The outlying transmembrane helices are given as ribbons. The inner helices are given as a trace of CA atoms. Water molecules and several functionally important amino acids are shown explicitly*

favorable than of others. If the length of the hydrocarbon side chain in these residues is additionally taken into consideration one could expected Glu-334 and Glu-785 amino acids to play the major role in stabilizing the counter ions for a given MC structure.

An important question is how the affinity to cation changes along the channel. To answer it the energy profiles of moving Na^+ (at 1 Å step) along the axis of the channel with the ionized Glu-334 and Glu-785 (MC^{2-}) are calculated. The equilibrated structure of MC^{2-} (60 ps MD run) is used as a starting geometry. In calculations of interaction energies geometry optimization of [MC^{2-}...Na^+] complex structure is performed at each position of Na^+. Besides, one water molecule closest to Na^+ is deleted for each ion position. The energy of interaction is calculated as the difference between the potential energies of the complex and of separated reactants. The calculations render a large negative value for the total interaction energy of Na^+ with MC^{2-}. This energy includes contributions from peptide part and water molecules and its major part is provided by electrostatic interactions. The total energy has a relatively stable and irregular character along the MC axis (Fig.6), which shows that water molecules effectively screen ion-ion interactions inside MC. The plot of interaction energy of Na^+ with the peptide part of MC^{2-} show two characteristic minimums at the positions proximate to anionic sites. Ion-protein interactions demonstrate a deeper minimum at the position close to Glu-334 (10.0 Å) than at position that is closer to Glu-785 (12.0 Å). Some extra rise of the potential profiles is related to the Phe residues that stick inside the pore at the periplasmic side of the channel.

Next, the energies of binding of 1-3 Na^+ ions, ΔE_{bind} , are estimated for the channel configuration having ionized Glu-334 and Glu-785 amino acids. This is done using formula (1) in two ways. First, in calculations of the binding energies the energy differences in formula (1) are considered between the systems [MC^{2-} + (150-n)H_2O +nNa^+] and [MC^{2-} +(150-n) H_2O] (n=1,2,3), that present the configurations where n Na^+ ions reside in MC interior and stand at the infinite separation from MC in gas phase, respectively. All the structures are obtained from MD equilibrated and geometry minimized [MC^{2-} +150 H_2O] structure and subjected to further geometry minimization. In the treatment of [MC^{2-} + (150-n)H_2O +nNa^+] complexes one water molecule is deleted for each occluded ion from a position that is closest to a given Na^+ at the channel interior. The structures of [MC^{2-} +(150-n) H_2O] systems are obtained from the [MC^{2-} +150 H_2O] structure by deleting the outlying n water molecules most weakly bound with MC. ΔE_{bind} has its lowest value (-76.7 kcal/mol) for the binding of 1 ion and rises upon sequential addition of two extra ions up to the value of -60.0 kcal/mol per ion (Table 2). While grasping some important features of the model the given calculations of ΔE_{bind} correspond to the gas phase case and are not expected to provide correct numerical estimates of binding

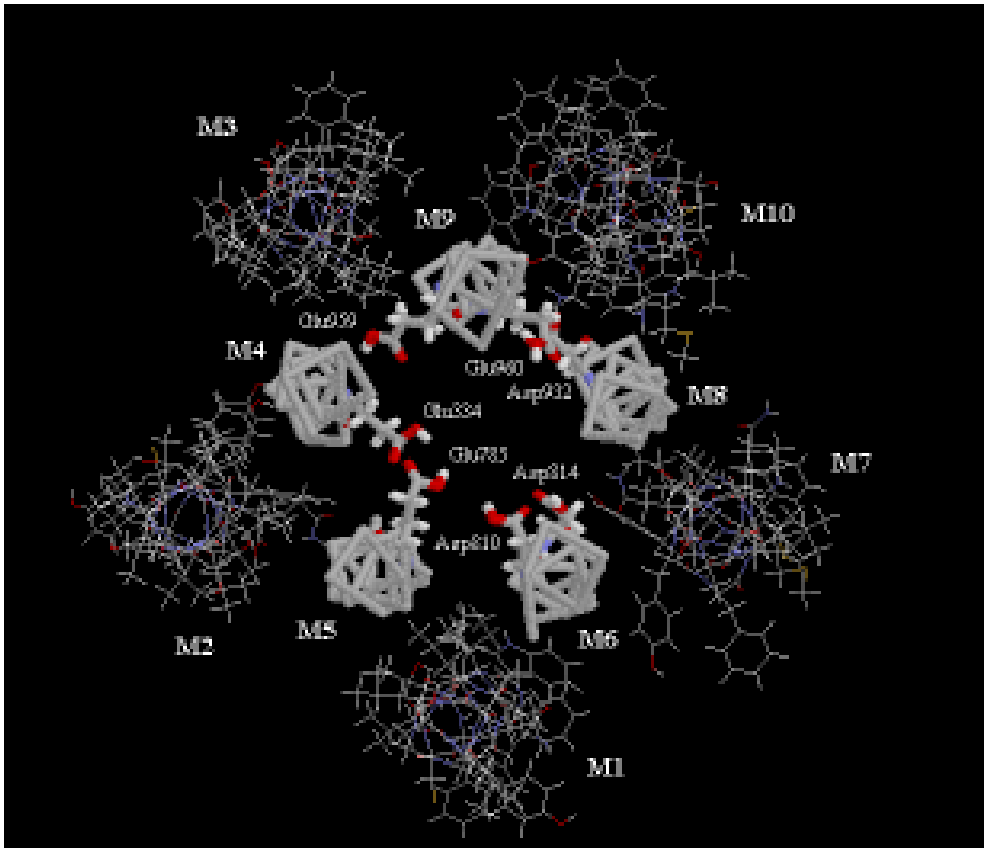

Figure 5b *Top view (from the extracellular space) of equilibrated MC structure. The outlying transmembrane segments are given as a wire-frame structure. The inner helices are given as a trace of CA atoms. Explicit orientations of selected Glu and Asp amino acids with respect to pore interior are presented. No water molecules are shown.*

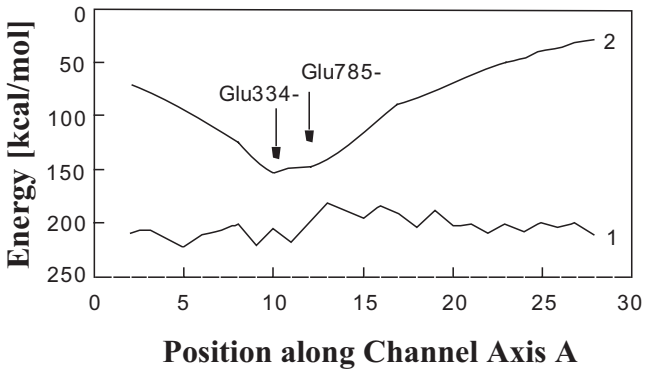

Figure 6 *Energy profiles of Na^+ ion in the MC having ionized Glu-334,785 residues. 1 - total energy, 2 - energy of electrostatic interaction with the protein part. Zero position corresponds to the intracellular side of the channel. Arrows indicate the positions of anionic residues along the channel axis*

energies in solution. Besides these calculations present the static approach since an important MD equilibration of the systems is missing here.

Second, the average structural properties of [MC^{2-} + 148H_2O +2Na^+] and [MC^{2-} + 147H_2O +3Na^+] complexes are considered along their MD trajectories. The equilibrated structure of MC^{2-} is taken as a starting one. 20 ps period is taken for system equilibration and 40 ps for data collection. In the complex with 2Na^+ the average distance between cations equals 3.62 Å, between cations and the negatively charged oxygen atoms of Glu-334 and Glu-785 - 2.37 and 2.24 Å, respectively. In the complex with 3Na^+ the average distances between cations equal 3.58, 4.07, and 6.03 Å, between the central cation and oxygen atoms of Glu-334 and Glu-785 - 2.31 and 2.29 Å, respectively. Although the absolute values of these distances reflect to a large extent the properties of the force field, still they show that in the complex with 3Na^+ the cations do not stand in one line along the channel axis, but rather form a triangle. The binding energies of these complexes are estimated here using formula (1) for the averaged energy contributions and taking the system [MC^{2-} + 150H_2O] as a reference one. These treatment corresponds to mutation of the water molecules into Na^+ ions inside the MC. As in case of static calculations the energy of the system corresponds basically to the gas phase treatment and lacks several important terms that are coming from the long-range electrostatic interactions of ions with an aqueous and lipid environment and from the induced dipoles interactions [29,30]. In the consistent approach the ΔE_{bind} calculated from MD averages should be compared with the energy difference of solvation energies of H_2O molecules and Na^+ ions considering the corresponding thermodynamic cycle (see ref. [29] for discussion). The latter difference can be estimated as 88.0 kcal/mol (per one ion) using solvation data of refs. [31,32]. The estimated value of the missing long-range ionic solvation energy terms in the treatment of [MC^{2-} + (150-n)H_2O +nNa^+] systems equal ~ -20 kcal/mol [29,30]. Adding it to the calculated value of ΔE_{bind} = -69.8 kcal/mol finally makes the overall binding of 3 Na^+ ions within a given model slightly exothermic relative to the reference energy of 88.0 kcal/mol in water.

Discussion

The given study does not involve determination of the unique 3-D structure that results from a protein folding under physiological conditions. It should be rather considered as an attempt of predicting the MC topology, building the structural model and estimating electrostatic properties of the resulting structure. Here, the membrane part of the α-subunit of Na,K-ATPase is modeled as a regular pentameric bundle of α-helices with an equal length which is a regular approach in ion channel studies but of course presents a crude approximation. 10-helix experimentally supported MC composition is assumed. The resulting pentagonal model is proposed considering the size of the pore, hydrophilic properties of the pore walls, geometrical arrangement of intersegment loops.

Unlike many passive ion channels with a well defined rigid pores Na,K-ATPase is an active transporter that undergoes deep conformational changes in order to make ion flux directed in and out of a cell. This could require a greater conformational mobility of its transmembrane helices compared to passive ion channels. The nature of these conformational changes isn't clear and it's hard to estimate how flexible in this respect is the given model. One possibility of such conformational transition follows from the given model and involves rotation of M4 or M5 helices (coupled with the conformational changes at the adjacent regulatory site due to ATP hydrolysis). In this way one of the corresponding Glu residues is moved out of the pore and the pore changes its affinity to cations. In general the requirement of nonintersection of intersegment loops used in model building ruled out the structures that could be considered as more strained and rigid. Also, in case of Na,K-ATPase the rule of a greater conservation among protein isoforms of amino acids belonging to the pore compared with membrane buried amino acids [13] should be applied when both E1 and E2 active conformations are taken into consideration. And there's still not enough data to apply this rule in present work, since here only the configuration with the maximal expected affinity to Na^+ ions (analogue of E1 conformation) is modeled. But the definite conclusion coming from sequence alignment is that most of acidic Asp and Glu amino acids belonging to the pore interior in this model are conserved. This supports the way the helices were assigned to the pore.

Several immediate results concerning the role of Glu and Asp residues follow from the proposed model. For the equilibrated MC structure only the side chains of Glu-334, Glu-785, Asp-810, and Asp-814 amino acids protrude into the channel pore. Glu-334 and Glu-785 residues are expected to be more efficient than Asp-810 and Asp-814 in binding positive counter ions according to calculated relative energies of

the ionized states and due to a longer amino acid hydrocarbon chain. This helps to understand the experimental data on the important role of these two Glu amino acids in binding ions both in E1 and E2 conformations [9,10]. The side chains of Glu-759 and Glu-760 amino acids are oriented at approximately 100 deg relative to each other (for a view along the M9 helix axis, Fig.5b). For a given pentagonal arrangement of membrane helices the Glu-759 and Glu-760 residues belong to the walls of the pore. Thus, they might be important for providing the favorable polar environment for the passing ions, but are not able to ensure strong binding with them in the same manner, as Glu-334 and Glu-785 do. This explains the existing controversy in experimental results, when some findings predict the important role of the Glu-759 and Glu-760, while some show that these amino acids have only a minor role in the ion binding [9,10b,c].

The modeling of ion binding is performed for the channel state with the ionized Glu-334 and Glu-785 amino acids since two negatively charged carboxy groups within the pore are sufficient for binding of 3 Na^+ ions. These particular residues are taken due to expected important role in cation binding. It is interestingly to note that in the given channel structure these residues are spatially close to each other and are located in the part of MC that is closer to the cell interior. Glu-334 stands at 10 Å and Glu-785 at 12 Å from the intracellular edge of MC. The other acidic groups also tend to be located closer to the intracellular side. It is not immediately clear how important this could be for the ion transport across membrane. Besides the positions of acidic residues could vary in a more sophisticated model where the structure of intersegment loops is taken into account. The calculated binding energies of Na^+ ions are not expected to give rigorous quantitative results due to neglect of important interactions with membrane and water surrounding. But despite of qualitative nature the straightforward calculation of binding energies with the model channel cluster might be useful in estimating the changes of the capacity of pore interior to bind several ions upon mutations of its structure.

Supplementary material The pdb file of the equilibrated and minimized structure of Na,K-ATPase channel and the table multiple alignment of transmembrane segments are available as Supplementary material.

Acknowledgement The financial support for this work came from Russian Fund for Fundamental Research (grant 04-48467). VL gratefully acknowledges the stipend from Deutscher Akademischer Austauschdienst along with the support from the Chemistry Department of the University of Paderborn, Germany. Discussions and cooperation with Gregor Fels and Larisa Vasilets are most appreciated by VL.

References

1. Stein,W.D. *Transport and Diffusion across Cell Membranes*, Academic: Orlando, San Diego, New York, 1986.
2. (a) Mohraz, M.; Simpson,M.V.; Smith, P.R. *J. Cell Biol.* **1987**, *105*, 1. (b) Skriver, E.; Kaveus, U.; Hebert, H.; Maunsbach, A.B. *J. Struct. Biol.* **1992**, *108*, 176.
3. Repke, K.R.H.; Schon, R. *Biol. Rev. Cambridge Philosophical Soc.* **1992**, *67*, 31.
4. Modyanov, N.N.; Vladimirova, N.M.; Gulyaev, D.I.; Efremov, R.G. In *Ion-Motive ATPases: Structure, Function and Regulation*, Scarpa, A.; Carafoli, E.; Papa,S., Eds.; Annals N.Y. Ac. Sci.: 1992, 671, pp.134-146.
5. Sweadner,K.J.; Arystarkhova,E. In *Ion-Motive ATPases: Structure, Function and Regulation* Scarpa, A.; Carafoli, E.; Papa,S., Eds.; Annals N.Y. Ac. Sci.: 1992, 671, pp.217-227.
6. (a) Capasso, J.M., Hoving, S.; Tal, D.M.; Goldshleger, R.; Karlish, S.J.D. *J. Biol. Chem*. **1992**, *267*, 1150. (b) Karlish, S.J.D.; Goldshleger, R.; Tal, D.M.; Capasso, J.M.; Hoving, S.; Stein, W.D. *Acta Physiologica Scandinavica* **1992**, *146*, 69. (c) Karlish, S.J.D.; Goldshleger, R.; Jorgensen, P.L. *J. Biol. Chem*. **1993**, *268*, 3471. (d) Arguello, J.M.; Kaplan, J.H. *J. Biol. Chem.* **1994**, *269*, 6892. (e) Arystarkhova, E.; Gibbons, D.L.; Sweadner, K.J. *J. Biol. Chem*. **1995**, *270*, 8785.
7. Vasiletz, L.; Schwarz, W. *Biochim. Biophys. Acta* **1993**, *1154*, 201.
8. (a) Antolovic, R.; Bruller, H.J.; Bunk, S.; Linder, D.; Schoner, W. *Eur. J. Biochem*. **1991**, *199*, 195. (b) Homareda, H.; Nagano, Y.; Matsui, H. *FEBS Lett*. **1993**, *327*, 99. (c) Ning, G.; Maunsbach, A.B.; Lee, Y.J.; Moller, J.V. *FEBS Lett*. **1993**, *336*, 521. (d) Larin, D.I.; Shakhparonov, M.I.; Ortiz, E.; Kostina, M.B.; Modyanov, N.N. *Biologicheskie Membrany* **1994**, *11*, 605.
9. Vasiletz, L.A.; Schwarz, W. *Cell Physiol. Biochem*. **1994**, *4*, 81.
10. (a) Canessa, C.M.; Horisberger, J.D.; Louvard, D.; Rossier, B.C. *EMBO J*. **1992**, *11*, 1681. (b) Vanhuysse, J.W.; Jewell, E.A.; Lingrell, J.B. *Biochemistry* **1993**, *32*, 819. (c) Lingrel, J.B.; Vanhuysse, J.; Obrien, W.; Jewellmotz, E.; Askew, R.; Schultheis, P. *Kidney Intern*. **1994**, *45*, S32. (d) Kunztweiler, T.A.; Wallick, E.T.; Johnson, C.L.; Lingren, J.B. *J. Biol. Chem*. **1995**, *270*, 2993. (e) Asano, S.; Tega, Y.; Konishi, K.; Fujioka, M.; Takeguchi, N. *J. Biol. Chem*. **1996**, *271*, 2740.
11. Schwarz, W.; Vasiletz, L.A. *Cell. Biol. International* **1996**, *20*, 67.
12. Popot, J.L. *Curr.Opin. Struct. Biol*. **1993**, *3*, 532.
13. Von Heijne, G. *Annu. Rev. Biophys. Biomol. Struct*. **1994,** *23*, 167.
14. (a) Pullman, A. In *Theoretical Biochemistry & Molecular Biophysics*, Beveridge, D.L.; Lavery, R., Eds.; Adenine: 1990, pp. 337-348. (b) Eisenman, G., Alvarez, O. In *Biomembrane Structure & Function - The State of the Art*, Gaber, B.P.; Easwaran, K.R.K., Eds.; Adenine: 1992, pp. 321-351. (c) Adams, P.D.; Arkin, I.T.; Engelman, D.M.; Brunger, A.T. *Nature Struct. Biol*. **1995**, *2*, 154. (d) Sansom, M.S.P.; Sankararamakrishnan, R.; Kerr, I.D. *Nature Struct. Biol*. **1995**, *2*, 624. (e) Khutorsky, V. *Biophysical J*. **1996**, *71*, 2984. (f) Hucho, F.; Tsetlin, V.I.; Machold, J. *Eur. J. Biochem*. **1996**, *239*, 539. (g) Grice,

A.L.; Kerr, I.D.; Sansom, M.S.P. *FEBS Lett*. **1997**, *405*, 299.
15. Luzhkov V.B., 11 CIC-Workshop, *Information und Wissen am Arbeits- und Ausbildungplatz des Chemikers*, Paderborn, Abstracts, 1996, p. 27.
16. Kawakami, K.; Noguchi, S.; Noda, M.; Takahashi, H.; Ohta, T.; Kawamura, M.; Nojima, H.; Nagano, K.; Hirose, T.; Inayama, S.; Hayashida, H.; Miyata, T.; Numa, S. *Nature* **1985**, *316*, 733.
17. Engelman, D.M.; Steitz, T.A.; Goldman, A. *Ann. Rev. Biophys. Biophys. Chem*. **1986**, *15*, 321.
18. Cserzo, M.; Bernassau, J.-M.; Simon, I.; Maigret, B. *J. Mol. Biol*. **1994**, *243*, 388.
19. Appel, R.D.; Bairoch, A.; Hochstrasser, D.F. *Trends Biochem. Sci*. **1994**, *19*, 258.
20. Corpet, F. *Nucl. Acid. Res*. **1988**, *16*, 10881.
21. *Insight II User Guide*, Biosym / MSI: San Diego, 1995.
22. Luzhkov V.B.; Surkov N.F. *Biologicheskie Membrany* **1997**, in press.
23. Dauber-Osguthorpe, P.; Roberts, V.A.; Osguthorpe, D.J.; Wolff, J.; Genest, M.; Hagler, A.T. *Proteins: Structure, Function and Genetics* **1988**, *4*, 31.
24. Warshel A.; Russel S.T. *Quart. Rev. Biophys*. **1984**, *17*, 283.
25. Edelman,J. *J.Mol.Biol*. **1993**, *232*, 165.
26. Brandl, C.J.; Deber, C.M. *Proc. Nat. Ac. Sci. USA* **1986**, *83*, 917.
27. Smart, O.S.; Breed, J.; Smith, G.R.; Sansom, M.S.P. *Biophys. J*. **1997**, *72*, 1109.
28. Gevondyan, N.M.; Gavrilyeva, E.E.; Gevondyan, V.S.; Grinberg, A.V.; Modyanov, N.N. *Biologicheskie Membrany* **1994**, *11*, 598.
29. Åqvist, J.; Warshel, A. *Biophys.J. Biophys. Soc*. **1989**, *56*, 171.
30. Luzhkov, V.; Warshel, A. *J. Comput. Chem*. **1992**, *13*, 199.
31. Jorgensen, W.L.; Chandrasekhar, J.; Madura, J.D. *J. Chem. Phys*. **1983**, *79*, 926.
32. Rashin, A.A.; Honig, B. *J.Phys. Chem*. **1985**, *89*, 5588.